RECENT RESULTS FROM HERMES*

M. Ruh

On behalf of the HERMES Collaboration

Albert–Ludwigs–Universität Freiburg, Fakultät für Physik
Hermann–Herder–Straße 3, 79104 Freiburg, Germany

(Received March 30, 1998)

The study of the spin structure of the nucleon is the primary goal of the HERMES experiment. In 1995, the first year of the experiment, the neutron structure function g_1^n was measured using a polarised ^{3}He target. Additionally, semi-inclusive hadron and pion asymmetries were extracted from ^{3}He. In 1996/97 a polarised hydrogen target was employed and preliminary results of the inclusive asymmetry as well as semi-inclusive hadron and pion asymmetries are presented. Preliminary results from the HERMES unpolarised physics program are shown including the valence quark distribution ratio $d_v(x)/u_v(x)$, the flavour asymmetry of the light quark sea, measurements of fragmentation functions and the decay angular distributions of ρ^0 mesons produced in exclusive deep inelastic electro-production.

PACS numbers: 14.20.Dh, 14.65.–q

1. Introduction

The total angular momentum of the nucleon can be written as the sum of contributions from quarks, gluons and orbital angular momenta

$$\frac{1}{2} = \frac{1}{2}\Delta\Sigma + \Delta L_q + \Delta g + \Delta L_g \,, \tag{1}$$

where, neglecting heavy quarks,

$$\Delta\Sigma = \Delta u + \Delta d + \Delta s \tag{2}$$

* Presented at the Cracow Epiphany Conference on Spin Effects in Particle Physics and Tempus Workshop, Cracow, Poland, January 9–11, 1998.

is the contribution from quark spins, Δg is the gluon contribution and ΔL_q, ΔL_g are those from angular momenta carried by quarks and gluons [33]. Here, each Δq_f refers to the sum of quark and anti-quark distributions with flavour f. It has been shown [26] that $\frac{1}{2}\Delta\Sigma + \Delta L_q \to \sim \frac{1}{4}$ and $\Delta g + \Delta L_g \to \sim \frac{1}{4}$ in the limit $Q^2 \to \infty$.

Up to the present, essentially all experiments have focused on the measurement of $\Delta\Sigma$. The current value from the combined world data is $\Delta\Sigma = 0.27 \pm 0.04$ at $Q^2 = 3$ GeV^2 [17] with the conclusion that the contribution of quark spins to the nucleon spin amounts to about 40% of the value expected from the relativistic quark model [33]. Furthermore, the contributions of the individual quark flavours are found to be $\Delta u = 0.82 \pm 0.03$, $\Delta d = -0.44 \pm 0.03$ and $\Delta s = -0.11 \pm 0.03$ at $Q^2 = 3$ GeV^2 based on inclusive structure function measurements in combination with the decay constants F and D from weak decays [17]. More recently, the x–dependence of polarised valence and sea quark distributions has been extracted using semi-inclusive measurements [9]. Until now, nothing is experimentally known about Δg, ΔL_g and ΔL_q. Next–to–Leading Order (NLO) analyses based on currently available inclusive and semi-inclusive polarised data still yield a poorly constrained gluon distribution [19, 23, 38].

HERMES has been designed to address many of the open questions concerning the spin structure of the nucleon using a new experimental technique to measure spin–dependent deep inelastic scattering. Both, inclusive and semi-inclusive processes are measured with clean positron hadron separation and additional pion identification. Different to other experiments, HERMES makes use of polarised pure atomic gas targets of hydrogen, deuterium and ^{3}He. Hadron identification provides means of flavour tagging, which allows for a direct measurement of the polarised quark distributions $\delta q_f(x)$ using semi-inclusive data. Additionally, the question of quark polarisations in the Λ–hyperon is being investigated, and, for the first time, the question of the gluon polarisation will be addressed experimentally.

2. The HERMES experiment

The HERMES experiment [24] is located at the HERA positron–proton collider at DESY in Hamburg, Germany. The experiment is arranged such that the 27.5 GeV longitudinally polarised positron beam interacts with internal polarised gas targets without interference from the proton beam. The beam is self–polarised transverse to the beam plane by synchrotron radiation (Sokolov–Ternov Effect) [36]. Spin rotators provide longitudinal beam polarisation at the HERMES interaction region. Positron polarisations exceeding 50% are routinely achieved and measured using two independent Compton backscattering polarimeters.

The HERMES target consists of an open ended thin walled storage cell through which the circulating positron beam passes. Polarised pure atomic gas is injected into the cell. In 1995 a polarised ^{3}He target was used. In 1996/97 the experiment was performed with a polarised hydrogen target. The target densities are about 7.5×10^{13} atoms/cm^2 for hydrogen and 3.5×10^{14} atoms/cm^2 for ^{3}He. The typical target polarisation is 90% (50%) for the hydrogen (^{3}He) source. The gas target allows for a fast spin reversal on the time scale of 1 (10) minute(s) for hydrogen (^{3}He). The luminosities obtained are in the range of $4 - 30 \times 10^{31}$ nucleons/(cm$^2\cdot$ sec). Additionally, unpolarised targets of hydrogen, deuterium, ^{3}He and nitrogen with thicknesses up to 10^{15} atoms/cm^2 have been used with the maximum target thickness limited only by the impact on the lifetime of the stored positron beam.

The HERMES spectrometer was designed for measuring both inclusive and semi-inclusive processes. A schematic diagram of the apparatus is shown in Fig. 1. The spectrometer is a large acceptance detector, which consists

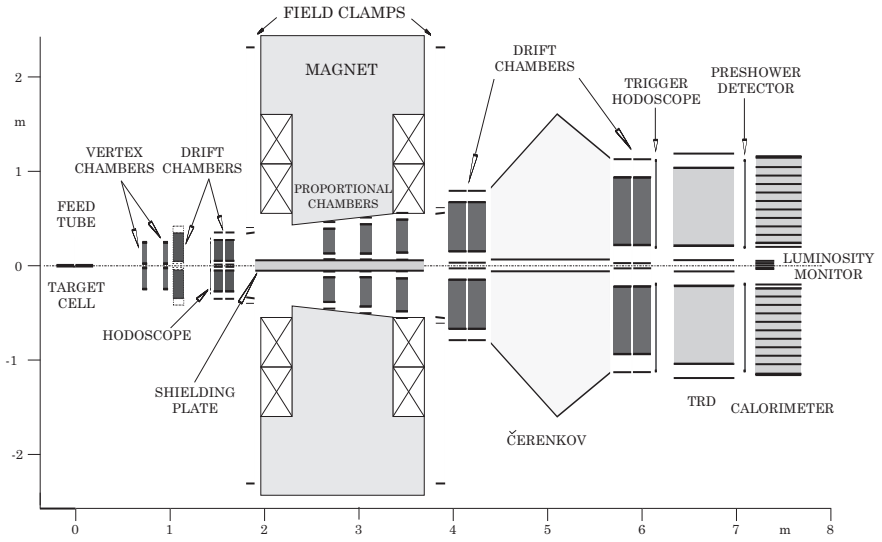

Fig. 1. Schematic diagram of the experimental apparatus (side view).

of two identical halves above and below the positron ring plane. It contains a dipole magnet with a bending strength of 1.3 Tesla·m and tracking chambers upstream the magnet, in the magnetic field and downstream the magnet providing charged particle tracking and momentum reconstruction. A positron momentum resolution of 1–2%, depending on the kinematics, and an average angular resolution of 0.6 mrad are achieved. Particle identifica-

tion is accomplished using a calorimeter, a preshower counter (a scintillator hodoscope preceded by 2 radiation length of Pb), six transition radiation detector modules and a N_2/C_4F_{10} threshold gas Čerenkov counter. This system provides clean positron hadron separation and additional pion identification. In 1995 (96/97) the threshold for pions to trigger the gas Čerenkov counter was 6 (4) GeV. The scattering angle acceptance of the spectrometer is $40 \leq \theta \leq 220$ mrad. The kinematic range accessible is $0.004 < x < 1$ and $0.2 < Q^2 < 20$ GeV^2. The relative luminosity is measured detecting Bhabha scattered target electrons in coincidence with the scattered positron.

3. Spin asymmetries and structure functions

3.1. Inclusive spin asymmetries

The basic features of the spin structure of the nucleon are characterised by the structure functions $g_1(x, Q^2)$ and $g_2(x, Q^2)$. These structure functions can be measured by deep inelastic scattering (DIS) of longitudinally polarised leptons on polarised nucleons. In lowest order QED[1] the cross section difference for opposite target polarisations is given by [25]

$$\frac{d^3\left[\sigma(\alpha)-\sigma(\alpha+\pi)\right]}{dx\ dy\ d\phi} = \frac{e^4}{4\pi^2 Q^2}\left\{\cos\alpha\left[a_1 g_1 - \frac{y}{2}\gamma^2 g_2\right] - \sin\alpha\cos\phi\ \sqrt{\gamma^2 a_2}\left[\frac{y}{2}\ g_1 + g_2\right]\right\}, \quad (3)$$

where Q^2 is the negative square of the virtual photon invariant mass, ν is the energy of the virtual photon, $y \overset{\text{lab}}{=} \nu/E$ and E is the energy of the incident lepton, $x \overset{\text{lab}}{=} Q^2/2M\nu$ is the Bjørken scaling variable and M is the nucleon mass. The quantity γ is defined by $\gamma = \sqrt{Q^2}/\nu$, $a_1 = 1 - y/2 - y^2\gamma^2/4$ and $a_2 = 1 - y - y^2\gamma^2/4$. For the definition of the angles α and ϕ see Fig. 2.

For a longitudinally polarised beam the structure functions g_1 and g_2 can be extracted from the cross section asymmetry measured for the target spin parallel and anti-parallel to the beam spin, $A_\parallel(x, Q^2)$, and the asymmetry $A_\perp(x, Q^2)$, which corresponds to the target polarisation perpendicular to the beam. The longitudinal polarisation asymmetry $A_\parallel$ is related to the virtual photon asymmetries $A_1(x, Q^2)$ and $A_2(x, Q^2)$ by [34]

$$A_\parallel = D(A_1 + \eta A_2), \quad (4)$$

[1] At HERMES energies the contributions from weak currents can be neglected.

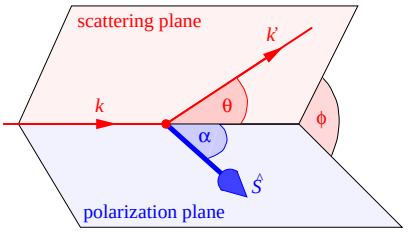

Fig. 2. Definition of scattering angles in polarised deep inelastic scattering. The four vectors of the incident and scattered lepton are denoted by $k = (E, \vec{k})$ and $k' = (E', \vec{k'})$. The lepton scattering angle is called θ. $\hat{S}$ gives the target polarisation direction and ϕ is the angle between the polarisation plane (defined by $\vec{k}$ and $\hat{S}$) and the scattering plane (defined by $\vec{k}$ and $\vec{k'}$). α is the angle between the beam momentum $\vec{k}$ and the target polarisation $\hat{S}$.

where the virtual photon depolarisation factor D and the kinematical factor η are given by

$$D = \frac{1-(1-y)\varepsilon}{1+\varepsilon R}\,, \quad \eta = \frac{2M\varepsilon\sqrt{Q^2}}{s\,[1-\varepsilon(1-y)]}. \tag{5}$$

The quantity $R(x,Q^2) = \sigma_{\mathrm{L}}/\sigma_{\mathrm{T}}$ is the ratio of longitudinal (σ_{L}) to transverse (σ_{T}) virtual photon absorption cross section, s is the lepton–nucleon centre–of–mass energy squared and ε is the degree of longitudinal polarisation of the virtual photon. The structure functions g_1 and g_2 can be expressed in terms of the asymmetries A_1 and A_2 and the unpolarised structure function $F_1(x,Q^2)$:

$$g_1 = \frac{F_1}{1+\gamma^2}\,(A_1 + \gamma A_2)\,, \tag{6}$$

$$g_2 = \frac{F_1}{1+\gamma^2}\left(\frac{A_2}{\gamma} - \gamma A_1\right). \tag{7}$$

The magnitude of A_2 is constrained by the positivity limit $A_2 \leq \sqrt{R}$ and was measured to be consistent with zero for the neutron and small in case of the proton [3,8,11]. Additionally, its contribution to g_1 and A_1 is suppressed by the kinematical factors γ and η, which are small in the kinematical region of our measurement. Neglecting γA_2 it follows from Eq. (6):

$$g_1 \simeq A_1\,\frac{F_1}{1+\gamma^2}\,, \tag{8}$$

which relates the structure function $g_1(x,Q^2)$ to the virtual photon asymmetry $A_1(x,Q^2)$. Furthermore, neglecting contributions from ηA_2, the asym-

metry A_1 can be expressed in terms of $A_\parallel$ following Eq. (4):

$$A_1 = \frac{A_\parallel}{D} - \eta A_2 \;\simeq\; \frac{A_\parallel}{D}\,. \tag{9}$$

In the Quark Parton Model (QPM) the polarised structure functions $g_{1/2}(x)$ are related to the quark spin distributions through

$$g_1(x) \;=\; \frac{1}{2}\sum_f e_f^2\;\delta q_f(x)\,, \tag{10}$$

$$g_2(x) \;=\; 0\,, \tag{11}$$

where $\delta q_f(x) = q_f^{\uparrow}(x) - q_f^{\downarrow}(x)$ and $q_f^{\uparrow(\downarrow)}(x)$ refers to the sum of quark and anti-quark distributions with flavour f and spin parallel (anti-parallel) to the nucleon spin and e_f is the quark charge in units of the elementary charge e. With the QPM expression for the unpolarised structure function $F_1(x) = 1/2\sum_f e_f^2\;q_f(x)$, where $q_f(x) = q_f^{\uparrow}(x) + q_f^{\downarrow}(x)$, it follows from Eqs. (6) and (7):

$$A_1(x) = \frac{g_1(x)}{F_1(x)} = \frac{\sum_f e_f^2\;\delta q_f(x)}{\sum_f e_f^2\;q_f(x)}\,. \tag{12}$$

Whereas in leading order QCD the polarised structure function g_1 decouples from the polarised gluon distribution, in NLO the polarised structure function g_1 is given as a convolution of coefficient functions with the polarised quark and gluon distributions. The calculation of the coefficient and splitting functions [29,31,32] (the latter needed to calculate the Q^2-dependence of the polarised parton distributions) during the last years has allowed a NLO QCD analysis of the scaling violations of the spin-dependent structure function $g_1(x, Q^2)$.

3.2. Semi-inclusive spin asymmetries

In semi-inclusive measurements a final state hadron is detected in coincidence with the scattered lepton. In the $\gamma^* N$ centre of mass system, after the absorption of the virtual photon, the struck quark and the target remnant will move roughly back to back and due to the confinement property of QCD will fragment into hadrons. The fragmentation process can be parameterised with fragmentation functions $D_{q_f}^h(z)$, which give the probability that a hadron h with energy fraction $z = E_h/\nu$ is produced after a quark of flavour f has been struck. At sufficiently large values of W hadrons associated with the struck quark (current fragmentation region)

will be kinematically confined to the forward region (large z, $x_F > 0$), while hadrons associated with the target remnant will be predominantly found in the backward region (small z, $x_F < 0$) with $x_F = 2p^*_\parallel/W$, where $p^*_\parallel$ is the hadron momentum component parallel to the virtual photon direction in the $\gamma^* N$ centre of mass frame. Hence, in the current fragmentation region one expects a large correlation between the flavour of the struck quark and the type of hadron produced, which allows for a flavour decomposition of the nucleon spin.

Provided factorisation of the scattering and the fragmentation process holds, the cross section for the production of a particular hadron h can be written

$$\sigma^h \propto \sum_f e_f^2 \; q_f(x) \cdot D^h_{q_f}(z) \; . \tag{13}$$

Defining the semi-inclusive structure functions

$$g_1^h(x,z) = \frac{1}{2} \sum_f e_f^2 \; \delta q_f(x) \cdot D^h_{q_f}(z) \tag{14}$$

and $F_1^h(x,z) = 1/2 \sum_f e_f^2 \; q_f(x) \cdot D^h_{q_f}(z)$, the semi-inclusive asymmetries can be expressed in the QPM in analogy to the inclusive one

$$A_1^h(x)\Big|_Z = \frac{\int\limits_Z dz \; g_1^h(x,z)}{\int\limits_Z dz \; F_1^h(x,z)} = \frac{\int\limits_Z dz \; \sum_f e_f^2 \; \delta q_f(x) \cdot D^h_{q_f}(z)}{\int\limits_Z dz \; \sum_f e_f^2 \; q_f(x) \cdot D^h_{q_f}(z)} \; . \tag{15}$$

The region Z, over which z is integrated, is determined by cuts on the hadron kinematics to select hadrons from the current fragmentation region. For a NLO QCD expression of the semi-inclusive structure function g_1^h see [18,19].

3.3. Extraction of inclusive and semi-inclusive spin asymmetries from data

The value of $A_1 \simeq A_\parallel/D$ is extracted from the measured count rates using the formula

$$\frac{A_\parallel}{D} = \frac{1}{D} \cdot \frac{N^- L^+ - N^+ L^-}{N^- L_P^+ + N^+ L_P^-} \; , \tag{16}$$

where N^+ (N^-) is the number of events for target spin parallel (anti-parallel) to the beam spin, $L^\pm$ are the dead time corrected luminosities for each target spin state, and $L_P^\pm$ are the dead time corrected luminosities weighted by the product of beam and target polarisations for each spin state. In the inclusive case the term *event* corresponds to the detection of a DIS lepton, whereas in the semi-inclusive case it refers to the detection of a hadron

from the current fragmentation region in coincidence with a DIS positron. For the DIS positron standard kinematic cuts of the form $Q^2 > 1$ GeV^2, $W^2 > 4$ GeV^2 and $y < 0.85$ are imposed.

3.4. Results on inclusive asymmetries and structure functions

The inclusive asymmetry A_1 and structure function g_1 is extracted from the measured asymmetry $A_\parallel/D$ using Eqs. (8) and (9) with $F_1 = F_2(1+\gamma^2)/\left[2x(1+R)\right]$. In order to determine the neutron structure function g_1^n from the measured asymmetry $A_1^{^3\mathrm{He}}$ corrections for nuclear effects and radiative corrections were applied [5]. The parameterisations for the unpolarised structure function $F_2(x,Q^2)$ and $R(x,Q^2)$ were taken from [13] and [39].

The results for A_1^n and g_1^n [5] are shown in Fig. 3 compared to the SLAC E154 experiment [4]. The dominant sources of the HERMES systematic error are the uncertainties in the polarisation measurements and in the calculations of nuclear and radiative corrections. Furthermore, the uncertainty on A_2^n was included into the systematic error of g_1^n. The first moment of g_1^n was evaluated at $Q_0^2 = 2.5$ GeV^2 assuming scaling behaviour of A_1^n. This assumption is consistent with existing data [2] and was checked in NLO QCD calculations to be valid within 5% inside the measured Q^2

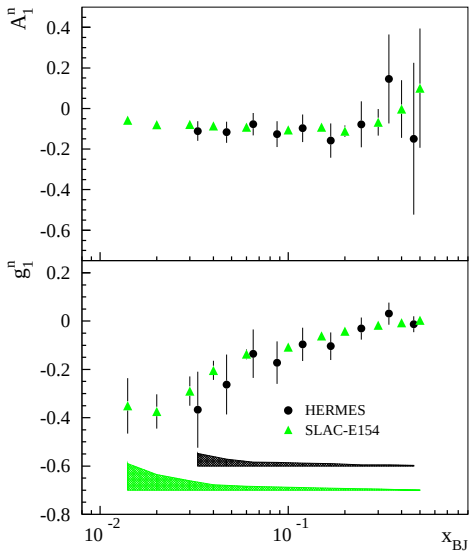

Fig. 3. The HERMES neutron asymmetry A_1^n and spin structure function g_1^n of the neutron compared to E154. The data are shown at the measured Q^2 of each experiment. The error bars are statistical uncertainties. The error bands show the systematic uncertainties.

range. The Ellis–Jaffe sum over the measured range is $\int_{0.023}^{0.6} g_1^n(x, Q_0^2)dx = -0.034 \pm 0.013(\text{stat.}) \pm 0.005(\text{syst.})$ in agreement with the results from SLAC [4, 11] and SMC [8].

The extraction of the proton asymmetry A_1^p was performed in the same way as for $A_1^{^3\text{He}}$. For the preliminary result shown in Fig. 4 it was assumed that $A_2^p = 0$. No background and radiative corrections have yet been applied. Radiative corrections were calculated to be typically 2% of the observed asymmetry. Note that the presented 1996 proton data have a relatively large normalisation error due to uncertainties in the target polarisation but represent only about 1/3 of the available proton data set.

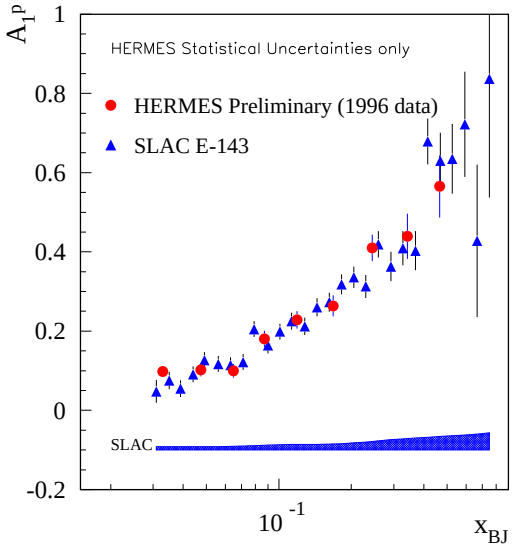

Fig. 4. The preliminary proton asymmetry A_1^p is shown at the measured Q^2 compared to E143. The error bars are statistical uncertainties. The error band shows the SLAC E143 systematic uncertainty.

3.5. Results on semi-inclusive asymmetries

Whereas in the inclusive case the count rate asymmetry of DIS positrons is extracted, in the semi-inclusive case it is the count rate asymmetry of hadrons measured in coincidence with a DIS positron. In addition a cut on z and x_F is imposed on the forwardness of the hadron.

The hadron asymmetries for both ^{3}He and hydrogen are shown in Fig. 5. For comparison also the inclusive asymmetries are shown. Fig. 6 shows the asymmetries for identified pions with momenta above 4 (6) GeV for

hydrogen (^{3}He). The presented 1996 hydrogen data cover about 1/3 of the available proton data set.

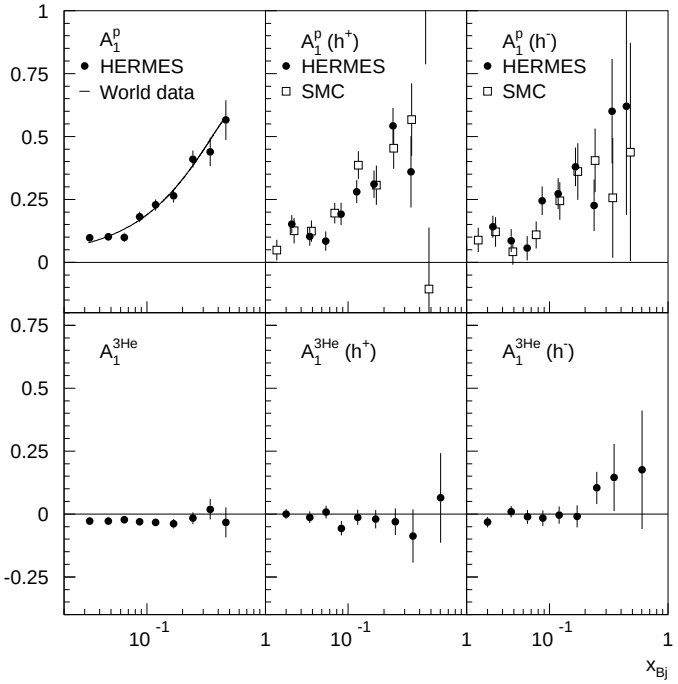

Fig. 5. The preliminary hadron asymmetries on the proton (top) and ^{3}He (bottom) compared to the inclusive ones. The hadron asymmetries on the proton are compared to SMC [9] in the HERMES kinematic range and the inclusive proton asymmetry is compared to world data. For the hadron asymmetries on the proton a cut of $z > 0.2$ and $x_F > 0.1$ (assuming the pion mass for all hadrons) was imposed on the forwardness of the hadron. For the hadron asymmetries on ^{3}He a cut of $z > 0.1$ was used.The error bars are statistical uncertainties.

The extraction of the polarised parton distributions from the inclusive and semi-inclusive asymmetries is currently being performed. Three different approaches are being pursued. Based on Eq. (13) the first approach uses the pion charge difference asymmetry measured on ^{3}He and hydrogen to extract the polarised valence distributions $\delta u_{\rm v}(x)$ and $\delta d_{\rm v}(x)$ [20]. This method needs to make use of isospin and charge conjugation invariance to reduce the number of independent fragmentation functions. The other two approaches rely on models of the fragmentation process. The so called *Purity* method uses the Lund model to calculate the fragmentation functions. The polarised quark distributions can then be unfolded from the measured asymmetries following Eq. (15). A second Monte Carlo method uses a po-

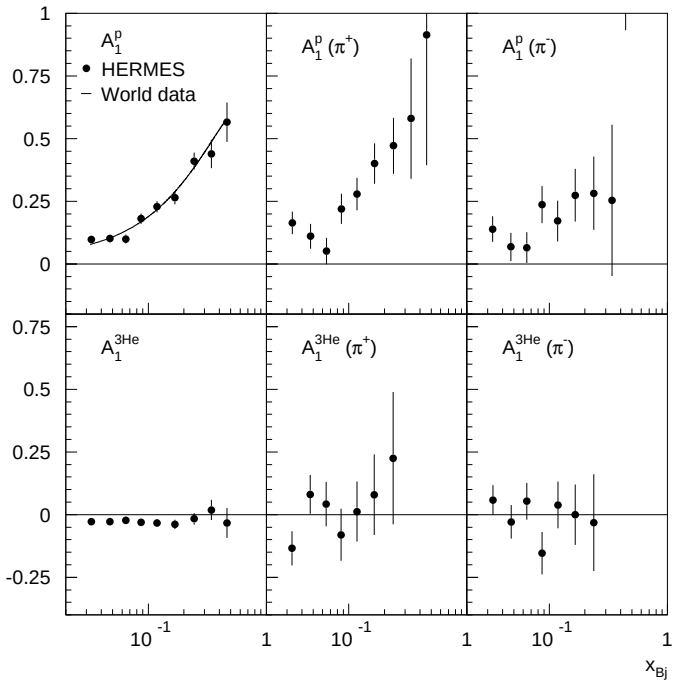

Fig. 6. The preliminary HERMES pion asymmetries on the proton (top) and ^{3}He (bottom) compared to the inclusive ones. The inclusive proton asymmetry is compared to world data. For the pion asymmetries a cut of $z > 0.2$ and x_F.0.1 was imposed on the forwardness of the pion. The error bars are statistical uncertainties.

larised DIS generator in combination with fragmentation models to predict the measured particle asymmetries. The shape of the polarised parton distributions incorporated into the DIS generator is then changed until the generated asymmetries fit to the measured ones.

4. Unpolarised physics

4.1. The ratio $d_v(x)/u_v(x)$

An example of the flavour tagging method comes from the unpolarised physics program with the measurement of the ratio of the unpolarised valence quark distributions $d_v(x)/u_v(x)$. Following Eq. (13) the cross section for the production of a particular hadron h, normalised by the inclusive cross section, $\sigma_{\rm DIS}$, can be written

$$\frac{1}{\sigma_{\rm DIS}(x)}\frac{d\sigma^h(x,z)}{dz} = \frac{1}{N^e(x)}\frac{dN^h(x,z)}{dz} = \frac{\sum_f e_f^2\, q_f(x)\cdot D_{q_f}^h(z)}{\sum_f e_f^2\, q_f(x)}\,, \qquad (17)$$

where N^e is the number of DIS events and N^h the number of coincident hadrons. With the measured yields of charged hadrons from a proton (p) and a deuterium (d) target the valence quark distribution ratio

$$\frac{d_{\rm v}(x)}{u_{\rm v}(x)} = \frac{4R^h(x) + [1-\Delta]}{4 + R^h(x)\cdot[1-\Delta]} \tag{18}$$

can be extracted, where

$$R^h(x) = \frac{N_d^{h^+}(x) - N_d^{h^-}(x)}{N_p^{h^+}(x) - N_p^{h^-}(x)} \cdot \frac{N_p^e(x)}{N_d^e(x)} \left[1 + \frac{F_2^n(x)}{F_2^p(x)}\right] - 1\,.$$

The quantity Δ depends on the u and d quark fragmentation functions into hadrons

$$\Delta = 1 - \frac{\int\limits_Z D_d^{h^-}(z) - D_d^{h^+}(z)\; dz}{\int\limits_Z D_u^{h^+}(z) + D_u^{h^-}(z)\; dz}\,, \tag{19}$$

and was estimated to be 0.3 ± 0.2 based on Monte Carlo simulations.

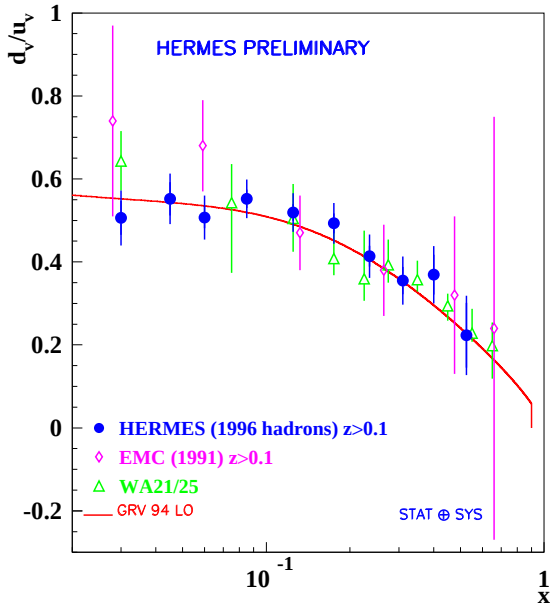

Fig. 7. The preliminary HERMES result on $d_{\rm v}(x)/u_{\rm v}(x)$ compared to the deep inelastic muon experiment EMC [14], the neutrino experiment WA21/25 [10,27] and the GRV94 leading order parametrisation [22], which was evolved to the HERMES mean Q^2 of 2.4 GeV^2.

Fig. 7 shows preliminary data for $d_{\rm v}(x)/u_{\rm v}(x)$ from the HERMES 1996 unpolarised running. The data points agree well with fits of $d_{\rm v}(x)/u_{\rm v}(x)$ to inclusive data and with measurements by other experiments proving that the flavour tagging method is applicable for the HERMES experimental conditions.

4.2. Measurement of fragmentation functions

HERMES has performed measurements of fragmentation functions of u and d quarks into pions [21]. This section presents results on the ratio of the unfavoured over the favoured pion fragmentation function $D^-(z)/D^+(z)$, where detector and acceptance corrections mostly cancel and comparisons with other experiments can be made.

The extraction of the fragmentation function ratio from the measured pion spectra is based on Eq. (17) and makes use of parameterisations of unpolarised parton distributions. Using isospin and charge conjugation invariance one obtains the following relations for the favoured D^+ and unfavoured fragmentation function D^-:

$$D^+ \equiv D_u^{\pi^+} = D_{\bar{d}}^{\pi^-} = D_{\bar{u}}^{\pi^-} = D_d^{\pi^+} , \tag{20}$$

$$D^- \equiv D_{\bar{d}}^{\pi^+} = D_u^{\pi^-} = D_{\bar{d}}^{\pi^-} = D_{\bar{u}}^{\pi^+} . \tag{21}$$

Assuming additionally for the fragmentation of s and $\bar{s}$ quarks into pions

$$D^- = D_s^{\pi^+} = D_{\bar{s}}^{\pi^-} = D_{\bar{s}}^{\pi^+} = D_{\bar{s}}^{\pi^-} , \tag{22}$$

the following formulae can be derived for the normalised differential pion rates for scattering off a proton target

$$\frac{1}{N_p^e}\frac{dN_p^{\pi^+}}{dz} = \frac{x}{9F_2^p}\left[(4u+\bar{d})D^+ + (4\bar{u}+d+s+\bar{s})D^-\right] , \tag{23}$$

$$\frac{1}{N_p^e}\frac{dN_p^{\pi^-}}{dz} = \frac{x}{9F_2^p}\left[(4\bar{u}+d)D^+ + (4u+\bar{d}+s+\bar{s})D^-\right] . \tag{24}$$

Analogous expressions can be given for deuterium and ^{3}He targets. Solving this system of equations for a particular target yields the fragmentation functions $D^-(z)$ and $D^+(z)$. For the unpolarised parton distributions the GRV NLO parameterisation in the $\overline{MS}$ renormalisation scheme was used [22]. A second extraction method has been performed with the results in agreement to the method described above. This second method uses the fact that on

an isoscalar target and neglecting sea quarks a simple expression for D^+ and D^- follows

$$D^{\pm} = \frac{1}{3N^e}\left[4\frac{dN^{\pi^{\pm}}}{dz} - \frac{dN^{\pi^{\mp}}}{dz}\right] . \tag{25}$$

However, gluons and sea quarks distort this simple picture and a Monte Carlo correction has to be applied.

The result for $D^-(z)/D^+(z)$ obtained with the first method using data on unpolarised proton, deuterium and ^{3}He targets is compared to the EMC measurement [12] in Fig. 8 and is found to be in good agreement. As D^+ and D^- are expected to evolve similarly with Q^2 a direct comparison of the measured ratios can be made.

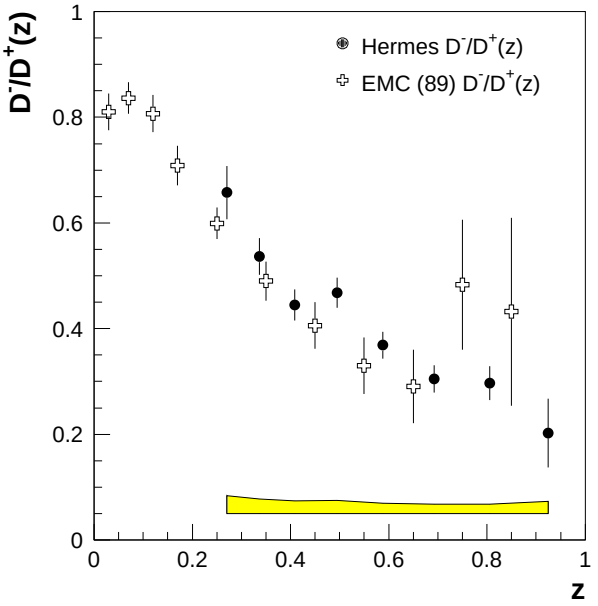

Fig. 8. Comparison of preliminary data on the ratio $D^-(z)/D^+(z)$ as measured with HERMES to the results of EMC [12]. The error band shows the systematic error of the HERMES measurement.

4.3. Flavour asymmetry of the light quark sea

The violation of the Gottfried Sum Rule measured by NMC [13]

$$S_{\rm G} \equiv \int_0^1 \frac{dx}{x}(F_2^p - F_2^n) = \frac{1}{3} + \frac{2}{3}\int dx\,[\bar{u}(x) - \bar{d}(x)] = 0.235 \pm 0.026 \neq \frac{1}{3} \tag{26}$$

indicates an excess of $\bar{d}$ over $\bar{u}$ quarks in the proton. The HERMES measurement of the light quark sea flavour asymmetry is based on Eq. (17). Assuming $\bar{u} = u_{\rm s}$ and $\bar{d} = d_{\rm s}$, the flavour asymmetry can be derived from the following ratio of oppositely charged pions produced from hydrogen and deuterium targets

$$\frac{\bar{d}(x) - \bar{u}(x)}{u(x) - d(x)} = \frac{\int\limits_Z dz\ f(z)\,[1 - r(x,z)] - [1 + r(x,z)]}{\int\limits_Z dz\ f(z)\,[1 - r(x,z)] + [1 + r(x,z)]}\,, \tag{27}$$

where

$$r(x,z) = \frac{N_p^{\pi^-}(x,z) - N_n^{\pi^-}(x,z)}{N_p^{\pi^+}(x,z) - N_n^{\pi^+}(x,z)}\,, \quad f(z) = \frac{3}{5} \cdot \left[\frac{1 + D^-/D^+(z)}{1 - D^-/D^+(z)}\right]$$

and $N^{\pi^\pm}(x,z)$ are the measured pion count rates. The fragmentation function ratio $D^-(z)/D^+(z)$ was taken from the HERMES measurement.

Fig. 9 (top plot) shows the light quark sea asymmetry $\left[\bar{d} - \bar{u}\right] / \left[u - d\right]$ compared to the GRV94 leading order [22] and CTEQ4(LQ) [30] parameterisations evolved to the appropriate HERMES Q^2. The only other published

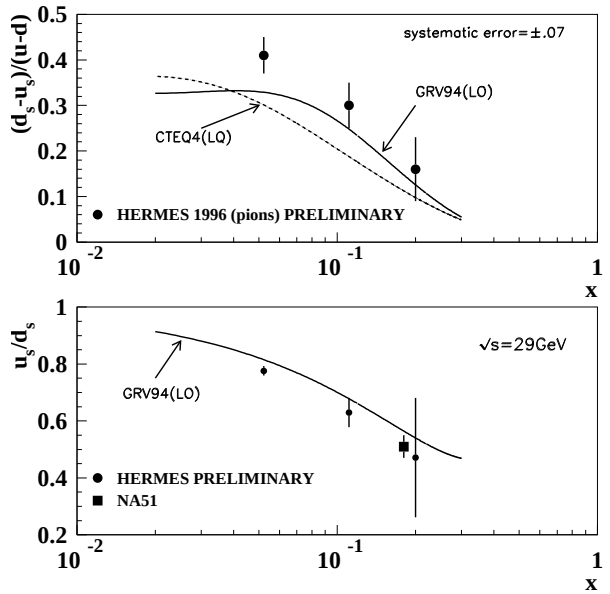

Fig. 9. Top plot: The light quark sea asymmetry, $\left[\bar{d}(x) - \bar{u}(x)\right] / \left[u(x) - d(x)\right]$ compared to the GRV94 leading order [22] and CTEQ4(LQ) [30] parameterisations. Bottom plot: The HERMES measurement converted to $\bar{u}/\bar{d}$ and compared to NA51 [15]. The HERMES error bars give the statistical uncertainty.

measurement comes from the NA51 experiment [15], which determined the ratio $\bar{u}/\bar{d}$. In order to compare with this experiment the GRV94 parameterisation has been used to convert the ratio $\left[\bar{d}-\bar{u}\right]/\left[u-d\right]$ into $\bar{u}/\bar{d}$. Furthermore, the HERMES data points were evolved to the kinematics of the NA51 experiment, which operated at a centre of mass energy of 29 GeV. The resulting $\bar{u}/\bar{d}$ is compared to NA51 in the lower plot of Fig. 9. Both measurements give a clear indication of the broken flavour symmetry of the light quark sea. In the near future the E866 experiment will publish additional data on the ratio $\bar{u}/\bar{d}$ in the range $0.03 < x < 0.35$.

4.4. Rho polarisation in exclusive $^3He\ (e,e'\rho^0)$

This section focuses on the decay angular distribution of ρ^0 mesons produced in diffractive, exclusive electro–production on ^{3}He. A discussion of the status of the ρ^0 production cross section and nuclear transparency measurements can be found elsewhere [37].

The $\rho^0(770) \to \pi^+\pi^-$ decay acts as an analyser of its spin state. Hence, the analysis of the decay angular distribution can be used to study the spin–dependent properties of the production process. Usually the ρ^0 decay angular distribution $W(\cos\theta,\phi,\Phi)$ is studied in a frame where the ρ^0 direction in the γ^*N centre of mass system is taken as the quantisation axis [28, 35]. The angle θ is defined as the polar angle and ϕ the azimuthal angle of the π^+ in the ρ^0 centre of mass system. The angle Φ is that between the ρ^0 production plane and the lepton scattering plane.

After integrating $W(\cos\theta,\phi,\Phi)$ over ϕ and Φ the distribution depends only on the density matrix element r^{04}_{00}, which gives the probability that the ρ^0 has helicity 0:

$$W(\cos\theta) = \frac{3}{4}\left[1 - r^{04}_{00} + (3r^{04}_{00} - 1)\cos^2\theta\right] . \tag{28}$$

Fig. 10 shows preliminary HERMES data for the $\cos\theta$ distribution from ρ^0 mesons produced in deep–inelastic electro–production from ^{3}He. Exclusive diffractive events were selected and an approximate acceptance correction was made. The curve represents a fit of function (28) to the data, which gives $r^{04}_{00} = 0.63 \pm 0.03 \pm 0.09$ at a mean Q^2 of 2.1 GeV^2. This value is compared to measurements by other experiments in Fig. 10 (bottom plot). An analysis for separate bins in Q^2 is currently being performed.

If the hypothesis of s–channel helicity conservation (SCHC) is valid, *i.e.* the assumption that the photon helicity is transfered to the vector meson, the decay angular distribution reduces to $W(\cos\theta,\psi)$, where $\psi = \phi - \Phi$ is the angle between the ρ^0 decay plane and the lepton scattering plane. After integration over $\cos\theta$ the distribution is given by

$$W(\psi) = \frac{1}{2\pi}\left[1 + 2\varepsilon r^1_{1-1}\cos 2\psi\right] , \tag{29}$$

where ε refers to the degree of longitudinal polarisation of the virtual photon. The parameter r^1_{1-1} is related to the probability that the ρ^0 has helicity ± 1. If one makes the additional assumption that unnatural parity exchange in the t-channel does not contribute [35], then $r^1_{1-1} = \frac{1}{2}[1 - r^{04}_{00}]$. Fig. 10 shows preliminary data on the ψ angular distribution using the same dataset as for the $\cos\theta$ distribution. The curve represents a fit according to Eq. (29), which was obtained assuming SCHC.

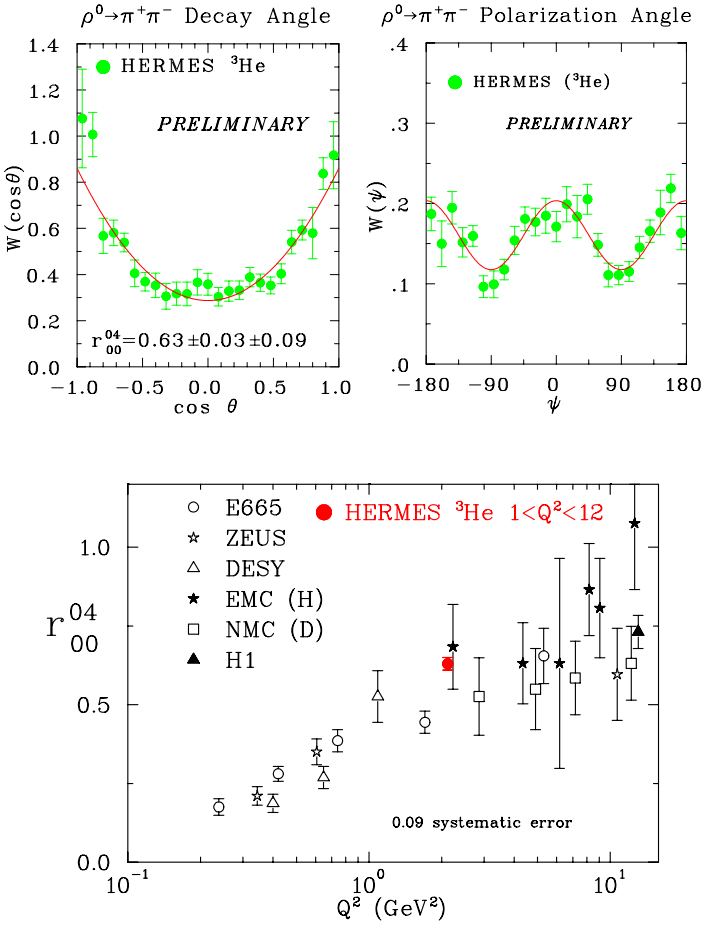

Fig. 10. Top plot: The decay angular distributions $W(\cos\theta)$ and $W(\psi)$ of ρ^0 mesons produced in diffractive, exclusive electro-production. Bottom plot: The density matrix element r^{04}_{00} compared to other experiments. All HERMES data shown are preliminary. The HERMES error bars show the statistical uncertainties.

5. Summary and outlook

The HERMES experiment has started data taking in 1995. The new experimental technique to measure spin–dependent deep inelastic scattering using an internal gas target with pure atomic species in the HERA storage ring works successfully. The result for the neutron structure function g_1^n obtained with a polarised ^{3}He target is consistent with data from other experiments. The preliminary result for the proton asymmetry A_1^p is also in good agreement with existing data. Preliminary results on semi-inclusive hadron and pion asymmetries were extracted from ^{3}He and hydrogen. The hadron asymmetries are in agreement with SMC, for the pion asymmetries HERMES has contributed the world's first measurement. The measurement of the valence quark distribution ratio $d_{\rm v}(x)/u_{\rm v}(x)$ from semi-inclusive data shows that the flavour tagging method can be applied successfully. First results on pion fragmentation functions measured at HERMES were presented and a measurement of the flavour asymmetry of the light quark sea was performed in the range $0.05 < x < 0.2$. The results are in agreement with the only other published measurement of $\bar{u}/\bar{d}$ at $x = 0.18$.

In 1998 HERMES will run with a polarised deuterium target. Currently, the threshold Čerenkov counter is converted to a Ring Imaging Čerenkov counter, which will allow for a clean p/K/π identification over the full momentum range. Furthermore, new components are installed for detection of D, D^* and J/ψ decay products to address the question of the gluon polarisation.

REFERENCES

[1] E143, K. Abe *et al.*, *Phys. Rev. Lett.* **75**, 25 (1995).
[2] E143, K. Abe *et al.*, *Phys. Lett.* **364**, 61 (1995).
[3] E143, K. Abe *et al.*, *Phys. Rev. Lett.* **76**, 587 (1996).
[4] E154, K. Abe *et al.*, *Phys. Rev. Lett.* **79**, 26 (1997).
[5] HERMES, K. Ackerstaff *et al.*, *Phys. Lett.* **B404**, 383 (1997).
[7] SMC, D. Adams *et al.*, *Phys. Lett.* **B336**, 125 (1994).
[8] SMC, D. Adams *et al.*, *Phys. Lett.* **B369**, 338 (1997).
[9] SMC, B. Adeva *et al.*, Preprint hep–ex/9711008, (1997).
[10] D. Allasia *et al.*, *Phys. Lett.* **B135**, 231 (1984).
[11] E142, P.L. Anthony *et al.*, *Phys. Rev.* **D54**, 6620 (1996).
[12] EMC, M. Arneodo *et al.*, *Nucl. Phys.* **B321**, 541 (1989).
[13] NMC, M. Arneodo *et al.*, *Phys. Lett.* **B364**, 107 (1995).
[14] EMC, J. Ashman *et al.*, *Z. Phys.* **C52**, 361 (1991).
[15] NA51, A. Baldit *et al.*, *Phys. Lett.* **B332**, 244 (1994).

[16] J. Ellis, R.L. Jaffe, *Phys. Rev.* **D9**, 1444 (1974).

[17] J. Ellis, M. Karliner, Preprint hep–ph/9601280, (1996).

[18] D. de Florian *et al.*, *Nucl. Phys.* **B470**, 195 (1996).

[19] D. de Florian *et al.*, Preprint hep–ph/9711440, (1997).

[20] L.L. Frankfurt *et al.*, *Phys. Lett.* **B230**, 141 (1989).

[21] P. Geiger, Measurement of Fragmentation Functions at HERMES, Ph.D. thesis, Universität Heidelberg (1998).

[22] M. Glück *et al.*, *Z. Phys.* **C67**, 433 (1995).

[23] M. Glück *et al.*, *Phys. Rev.* **D53**, 4775 (1996).

[24] HERMES Collaboration, Technical Design Report, DESY–PRC 93/06 (1993).

[25] R.L. Jaffe, *Comments Nucl. Part. Phys.* **19**, 239 (1990).

[26] X. Ji, *Phys. Rev. Lett.* **78**, 610 (1997).

[27] WA21, G.T. Jones *et al.*, *Z. Phys.* **C62**, 601 (1994).

[28] P. Joos *et al.*, *Nucl. Phys.* **B113**, 53 (1976).

[29] A.L. Kataev, V.V. Starshenko, *Mod. Phys. Lett.* **A10**, 235 (1995).

[30] H.L. Lai *et al.*, *Phys. Rev.* **D55**, 1280 (1997).

[31] S.A. Larin, J.A.M. Vermaseren, *Phys. Lett.* **B259**, 345 (1991).

[32] S.A. Larin, *Phys. Lett.* **B334**, 192 (1994).

[33] R.L. Jaffe, A. Manohar, *Nucl. Phys.* **B337**, 509 (1990).

[34] R.G. Roberts, *The structure of the Proton*, Cambridge University Press (1990).

[35] K. Schilling, G. Wolf, *Nucl. Phys.* **B61**, 381 (1973).

[36] A.A. Sokolov, I.M. Ternov, *Sov. Phys. Dokl.* **8**, 1203 (1964).

[37] G. van der Steenhoven, *Nucl. Phys.* **A622**, 31c (1997).

[38] M. Stratmann, Proceedings of the Workshop, DESY–Zeuthen, September 1–5 (1997).

[39] L. Whitlow *et al.*, *Phys. Lett.* **B250**, 193 (1990).